Taylor & Francis
Taylor & Francis Group

REPORT

OPEN ACCESS | Check for updates

# Impact of linker-drug on ion exchange chromatography separation of antibody-drug conjugates

Zhaorui Zhang, Shiyue Zhou, Linjie Han, Qunying Zhang, and Wayne A. Pritts

Process Analytical Chemistry, AbbVie Inc., North Chicago, IL, USA

**ABSTRACT**

Charge variants are important attributes of monoclonal antibodies, including antibody-drug conjugates (ADCs), because charge variants can potentially influence the stability and biological activity of these molecules. Ion exchange chromatography (IEX) is widely used for charge variants analysis of mAbs and offers the feasibility of fractionation for in-depth characterization. However, the conjugated linker-drug on ADCs could potentially affect the separation performance of IEX, considering IEX separation relies on surface charge distribution of analyte and involves the interaction between analyte surface and IEX stationary phase. Here, we investigated weak cation exchange chromatography (WCX) for its application in analyzing three ADCs (two broad distribution ADCs and an ADC with controlled conjugation sites) and the 2-drug/4-drug loaded species isolated from the two broad distribution ADCs using hydrophobic interaction chromatography. The major peaks in WCX profile were characterized via fraction collection followed by capillary electrophoresis-sodium dodecyl sulfate or peptide mapping. Results suggested that both the number of drug loads and conjugation sites could impact WCX separation of an ADC. The hypothesis was that the linker drugs could interfere with the ionic interaction between its surrounding amino acids on the mAb surface and column resin, which reduced the retention of ADCs on WCX column in this study. Our results further revealed that WCX brings good selectivity towards positional isomers, but limited resolution for different drug load, which causes the peak compositions of the two broad-distribution ADCs to be highly complex. We also compared results from WCX and imaged capillary isoelectric focusing (icIEF). Results showed that separation in icIEF was less influenced by conjugated linker drugs for the ADCs studied in this work, and better alignment was found between the two techniques for the ADC with controlled conjugate sites. Overall, this work provides insights into the complexity of WCX analysis of ADCs, which should be considered during method development and sample characterization.

## Introduction

Antibody-drug conjugates (ADCs) for cancer have recently become the focus of intense research and development efforts. ADC technology combines the advantage of the specificity of a monoclonal antibody (mAb) and the potency of a cytotoxic agent. The cytotoxic agents are usually linked covalently to the cysteine or lysine residue of a mAb via a chemical linker to form an ADC. For cysteine-linked ADCs, one common approach involves a two-step reaction. First, the interchain disulfide bonds are cleaved into free cysteines by partial reduction, and then cytotoxic drugs are conjugated to the antibody via a thiol-maleimide reaction.[1,2] Due to the complexity of this reaction and microheterogeneity of an antibody, a highly heterogeneous ADC molecule is expected, containing species not only with different numbers of drug loads but also with different conjugation sites. Non-reduced capillary electrophoresis-sodium dodecyl sulfate (CE-SDS), peptide mapping and middle-up liquid chromatography-mass spectrometry (LC-MS) analysis are commonly used techniques to identify conjugation sites in ADCs.[2–5] The possible positional isomers of ADCs conjugated using interchain disulfide bonds are illustrated in Table 1.

Charge heterogeneity is an important attribute for mAbs since it may affect both their *in vitro* and *in vivo* properties, and therefore characterization or comparability data are required to demonstrate the consistency in product quality for regulatory filings of antibody therapeutics.[6–10] Charge variants in mAbs are the result of multiple post-translational modifications and process-related degradation events, such as deamidation, oxidation, sialylation, incomplete N-terminal or C-terminal processing.[7,11–13] Charge-based separation techniques such as ion exchange chromatography (IEX) and capillary isoelectric focusing (cIEF) are commonly used to monitor these variants. Charge variants are referred to as acidic or basic species, as compared with the main species. Taking cation exchange chromatography (CEX) as an example, acidic variants are variants that elute earlier than the main peak and basic variants are those that elute later than the main peak. The elution order is reversed in anion exchange chromatography (AEX). In cIEF, acidic species are variants with lower apparent pI and basic species are those with higher apparent pI. In general, for antibody analysis, good agreement can be found between these two techniques, but there may be subtle differences due to different separation mechanisms. IEX depends on not only the overall charge of

**Table 1.** Positional isomers of ADCs conjugated using interchain disulfide bonds, with attached linker drugs indicated by red dots. Chain compositions under denaturing and nonreducing condition in CE-SDS are illustrated below each isomer. The possible species formed are L, H, LH, HH, LHH, and LHHL, where the indicated light (L) and heavy chains (H) are linked by the remaining interchain disulfide bond.

| DAR | Positional isomer | | | |
|---|---|---|---|---|
| 0 | E0 | | | |
| 2 | L, LHH<br>E2$_A$ | E2$_{H1}$ | E2$_{H2}$ | |
| 4 | L, LHH<br>E4$_{AA}$ | LHHL<br>E4$_{AH1}$ | LHHL<br>E4$_{AH2}$ | E4$_{HH}$ |
| 6 | L, HH<br>E6$_{AAH1}$ | L, LHH<br>E6$_{AAH2}$ | L, LHH<br>E6$_{AHH}$ | LH |
| 8 | L, HH<br>E8 | L, HH | L, H, LH | |
| | L, H | | | |

the mAb but also surface charge distribution, which affects the interaction between the molecule and the column resin. cIEF, on the other hand, separates the variants based only on the overall charge of each species. The differences between IEX and cIEF for antibody analysis have been previously reported.[8,11,14,15]

Since an ADC is made from a mAb, analysis of ADC charge variants would be expected by a regulatory agency to assure its quality. Due to the high complexity in ADCs, development of appropriate analysis methods can be very challenging.[16,17] There have been very few reports on charge-based methods for ADCs. cIEF[18] and capillary zone electrophoresis (CZE)[17] techniques have been described for charge variants analysis of ADCs. cIEF has gained its popularity in the industry for the analysis of an ADC since in general it allows for easier method development and gives a simpler separation profile compared to chromatographic techniques. New techniques, including microfluidic capillary electrophoresis-mass spectrometry (CE-MS)[19] and ultra-high voltage CE,[20] have also been developed for ADC analysis. Compared to electrophoresis-based techniques such as cIEF and CZE, IEX offers the capability of fractionation for further analysis of ADCs. However, the drugs on ADCs may affect the separation in IEX besides the charge heterogeneity on the antibody itself, since the mechanism of IEX involves interaction between analyte surface and stationary phase. This complexity of IEX for ADC analysis has been acknowledged in previous reports but was not well understood.[17,18] Better understanding

of how linker-drug affects IEX separation of ADC can help researchers choose suitable technique for charge variants analysis of ADCs and better use IEX as a tool to facilitate sample characterization.

Here, we analyzed three different ADCs and each drug load species isolated by hydrophobic interaction chromatography (HIC) by weak cation exchange chromatography (WCX) and compared the results with those from imaged capillary isoelectric focusing (icIEF). Selected WCX peaks from each ADC were further fractionated and characterized by non-reduced CE-SDS or peptide mapping to understand the factors that contribute to the WCX separation of ADCs.

## Results

### Purified E2 and E4 species

E2 and E4 fractions in HIC were collected from the broad distribution mixture of ADC1 and ADC2 for further analysis. Each fraction was then re-analyzed by HIC to confirm the purity (Figure 1). From HIC analysis, the E2 and E4 fractions purities are 98.7% and 90.2% for ADC1, and 96.5% and 91.7% for ADC2, respectively.

### Weak cation exchange chromatography

Broad distribution of ADC1 and ADC2, purified E2 and E4 species of ADC1 and ADC2, along with mAb1 and mAb2 were analyzed by WCX. WCX elution gradients were optimized for each ADC. WCX results of mAb1 and ADC1 (E2, E4, and broad distribution) are demonstrated in Figure 2. The charge distribution for ADC1 E2 and E4 is assigned based on the results from CE-SDS, which are discussed below. Percentages of charge variants of ADC1 tested by WCX are listed in Table 2. From Figure 2a, only one major peak was observed for mAb1 with WCX, which was the main species of this mAb. Acidic species and basic species are labeled on the two sides of the main peak as demonstrated in Figure 2a. Comparing Figure 2b with Figure 2a, ADC1 E2 showed a similar profile to mAb1, but with an earlier elution time under the same gradient. An additional peak that eluted at ~13.5 min (labeled as F1) was observed before the main peak for ADC1 E2, which was identified as acidic species and is discussed below.

ADC1 E4 and ADC1 broad distribution, on the other hand, showed a dramatically different profile in WCX compared to the mAb1 and E2 species (Figure 2). Three major peaks were observed for ADC1 E4 in the WCX chromatogram (Figure 2c): two peaks eluted before the main peak of ADC1 E2, while one eluted at approximately the same time as the main peak. Note that there were less than 1% E2 species in the ADC1 E4 sample according to its HIC profiles. Thus, when we look at the WCX chromatogram of ADC1 broad distribution sample (Figure 2d), the most intense peak near 14.5 min could be a mixture of at least three components: 1) main peak of ADC1 E2; 2) the second main peak of E4 species; and 3) a portion of the acidic species of mAb1. Likewise, other peaks in the ADC1 broad distribution could also be mixtures of different charged species.
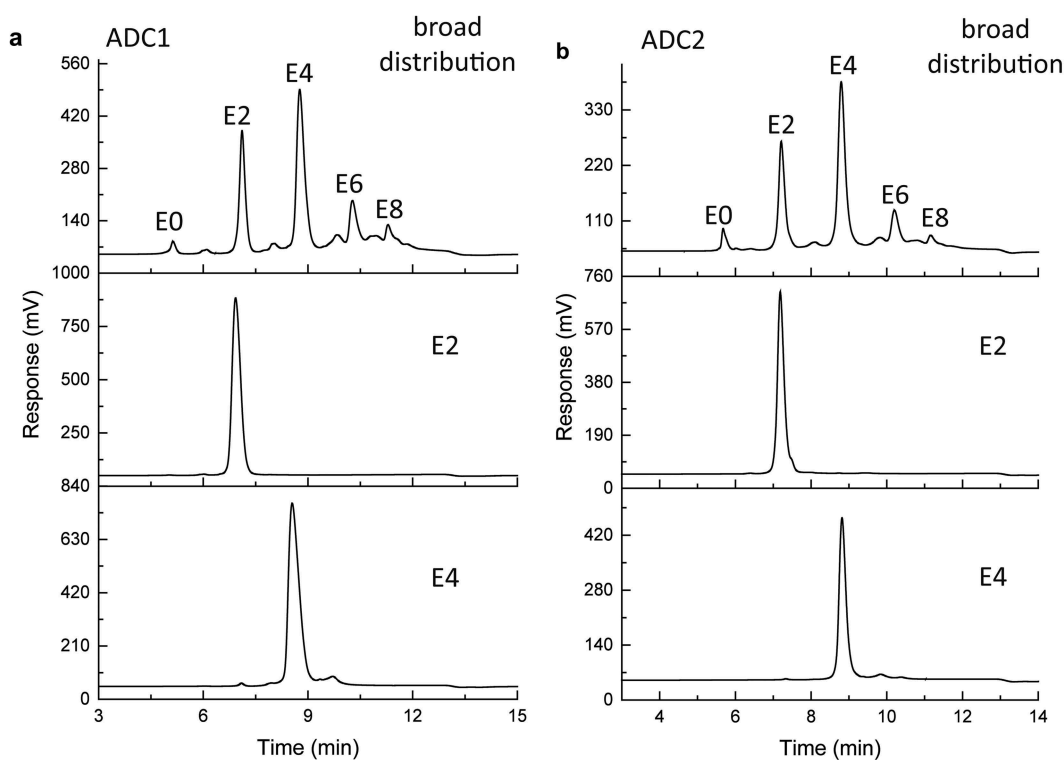
**Figure 1.** (a) HIC profile for ADC1 broad distribution (top), E2 (middle) and E4 (bottom); (b) HIC profile for ADC2 broad distribution (top), E2 (middle) and E4 (bottom).

WCX analyses of mAb2 and ADC2 (E2, E4, broad distribution) are demonstrated in Figure 3a-d. The WCX pattern was similar: E2 profiles looked similar compared to the mAb with shift in retention time; E4 as well as broad distribution gave very different chromatograms compared to mAb and E2 species. Comparing the chromatograms in Figure 3, again they demonstrate that WCX peaks for ADC2 with broad distribution could be mixtures of different charged species (e.g., acidic, main, basic species) from species with different drug loads (e.g., E0, E2, E4, E6, E8).

In order to identify major charge variants, WCX fractions were collected for ADC1, ADC2 and their HIC purified E2/E4, followed by CE-SDS and MS analysis.

## Capillary electrophoresis-sodium dodecyl sulfate (CE-SDS) analysis of WCX fractions

Under denaturing but nonreducing condition in CE-SDS, an ADC conjugated through interchain disulfide bonds dissociates into fragments based on the conjugation site, as illustrated in Table 1. WCX fractions collected from the E2 and E4 species of ADC1 and ADC2 were subjected to non-reduced CE-SDS for analysis. Due to sample complexity, WCX fractions were not collected for ADC samples with broad distribution.

As an example, CE electropherograms of ADC1 E4 and its three WCX fractions are shown in Figure 4. Figure 4a illustrates the three WCX fractions collected for ADC1 E4. During the conjugation step, certain interchain disulfide bonds in this ADC were reduced to create free cysteines. Once an interchain disulfide bond breaks, it can no longer hold the ADC together under a denaturing condition, such

as the CE-SDS condition. As a result, the ADC broke into fragments in the CE-SDS analysis. As demonstrated in Table 1, an E4 species can generate four possible positional isomers, $E4_{AA}$, $E4_{HH}$, $E4_{AH}$, and $E4_{HA}$. Under the CE-SDS condition, $E4_{AA}$ breaks down into fragments of L and HH; $E4_{HH}$ into LH fragments; $E4_{AH}$ and $E4_{HA}$ into L and LHH. $E4_{AH1}$ and $E4_{AH2}$ are not distinguishable by non-reduced CE-SDS. For ADC1 E4, five fragments were observed by non-reduced CE-SDS: L, H, LH, HH, and LHH. The most abundant fragments observed were L, LH, and HH, indicating $E4_{AA}$ and $E4_{HH}$ are the most abundant components in ADC1 E4, which is consistent with literature reports.[2,3] Fragment LHH can be contributed by $E4_{AH}$/$E4_{HA}$ and certain impurities with lower drug load, such as E2 and E3. Fragment H can be from impurities with higher drug load, such as E5. CE electropherograms of the three WCX fractions of ADC1 E4 are demonstrated in Figure 4c-e. In both Fraction 1 and 2, L and HH fragments dominated, indicating that both fractions contained mainly positional isomer $E4_{AA}$. The dominance of fragment LH in Fraction 3 indicated that Fraction 3 contained mainly $E4_{HH}$. $E4_{AH}$ was hardly seen, which is consistent with previous literature reports.[2,21]

Non-reduced CE analysis results of E2 and E4 species along with their WCX fractions for ADC1 and ADC2 are listed in Table 3. It is obvious that Fraction 1 and 2 of ADC1 E4 are more closely related to each other than to Fraction 3. Fragments from $E4_{AA}$ dominated in Fraction 1 and 2, while fragments from $E4_{HH}$ dominated in Fraction 3. The CE results clearly demonstrated that the positional isomers of ADC1 E4 were separated by WCX. In addition, both Fraction 1 and 2 have similar composition (mainly $E4_{AA}$)
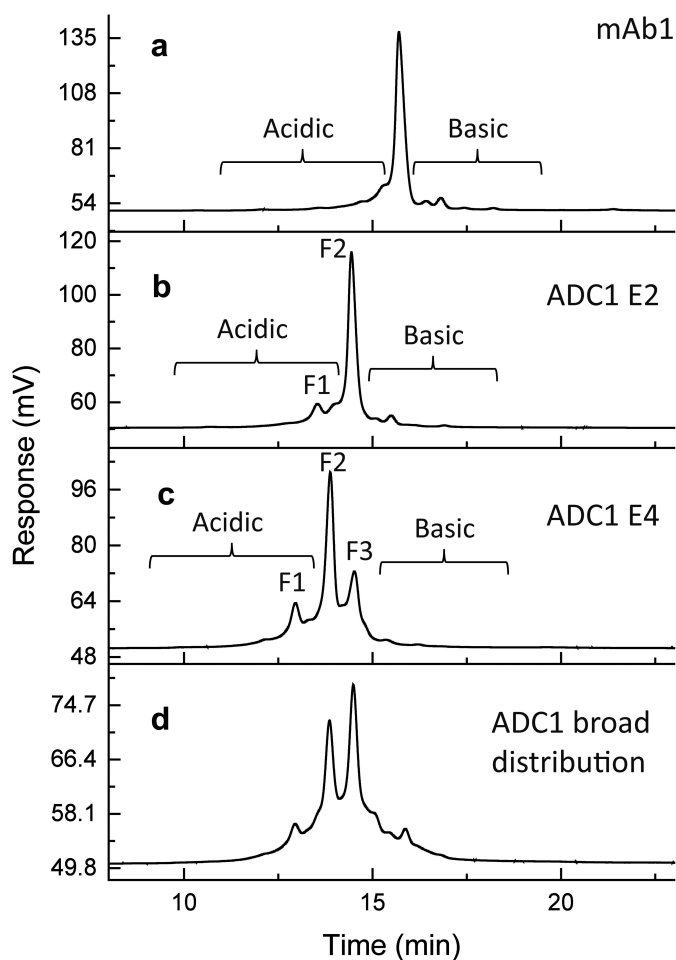
**Figure 2.** WCX chromatograms of (a) mAb1, (b) ADC1 E2, (c) ADC1 E4 and (d) ADC1 broad distribution in the same time domain, with charge variants assignment for mAb1, ADC1 E2, and E4. WCX fractions collected from ADC1 E2 and ADC1 E4 for subsequent analyses are illustrated. F1 = Fraction 1; F2 = Fraction 2; F3 = Fraction 3.

**Figure 3.** WCX chromatograms for (a) mAb2, (b) ADC2 E2, (c) ADC2 E4 and (d) ADC2 broad distribution. WCX fractions collected for subsequent analyses are illustrated. F1 = Fraction 1; F2 = Fraction 2.

**Table 2.** Percentage of charge variants in ADC1 tested by WCX and icIEF.

| Sample | WCX | | | icIEF | | |
|---|---|---|---|---|---|---|
| | %acidic | %main | %basic | %acidic | %main | %basic |
| mAb1 | 22.0 | 65.3 | 12.7 | 21.4 | 68.6 | 10.0 |
| ADC1 E2 | 25.8 | 62.1 | 12.2 | 27.6 | 60.6 | 11.8 |
| ADC1 E4 | 24.1 | 41.5 (F2), 18.6 (F3) | 12.1 | 33.8 | 58.3 | 7.9 |
| ADC1 BD | NA | NA | NA | 35.9 | 54.8 | 9.3 |

*BD: broad distribution

despite the fact that Fraction 1 eluted earlier. Based on this result, Fraction 1 was assigned as the acidic form of E4$_{AA}$ for integration purposes, and the integration result was compared with that from the icIEF test. Both Fraction 2 and 3 are considered as the main peaks of sample ADC1 E4 since they represent two different positional isomers.

For ADC1 E2, only L and LHH fragments (Figure S1) were observed in Fraction 1 by CE so there was mainly E2$_A$. However, the signal intensity was low in CE analysis due to the low concentration of Fraction 1; peak area percentages were thus not calculated. Fraction 2 was taken from the main peak in ADC1 E2. The CE result of Fraction 2 was compared against the result of overall ADC1 E2 sample to determine if there were any significant changes in fragments. Fraction 2 and the overall ADC1 E2 showed very similar fragment profiles, mainly L and
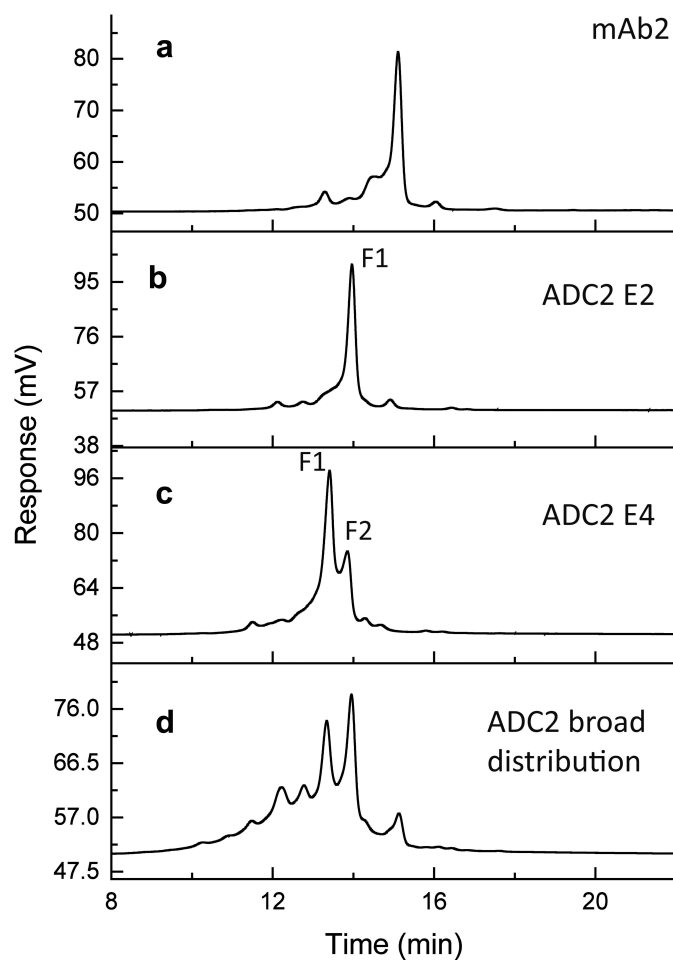
LHH fragments from E2$_A$. Since both Fraction 1 and 2 represented positional isomer E2$_A$, Fraction 1 was assigned as acidic form of E2$_A$ for comparison with the icIEF results. The amount of LHHL fragment was very low in CE (5.4% by peak area), which was mainly contributed by E2$_H$. E2$_H$ was not resolved in the WCX chromatogram of ADC1 E2.

For the E4 species of ADC2, non-reduced CE identified Fraction 1 as E4$_{AA}$ and Fraction 2 as E4$_{HH}$. For the E2 species of both ADCs, fragment distributions between the overall E2 sample and the fraction of the main peak are very similar, where mainly fragments from E2$_A$ were observed. The non-reduced CE results of E4 species and their WCX fractions in Table 3 demonstrated the capability of WCX to separate positional isomers in ADCs.

This further complicates the scenario in WCX separation of ADCs, as each positional isomer should have its own acidic and basic forms. For example, for the E4 species of ADC1 and ADC2 we tested, part of the acidic species in E4$_{HH}$ could coelute with the main peak of E4$_{AA}$. The separation of positional isomers in ADCs also explains why the WCX profiles of the three ADCs with broad distribution were so different from the profile of the mAb from which they originated. For a neutral linker-drug, such as maleimidocaproyl-valine-citrulline-monomethyl auristatin E (mc-vc-MMAE), the WCX separation of an ADC with broad distribution was not only based on the number of drugs loaded, but also on the
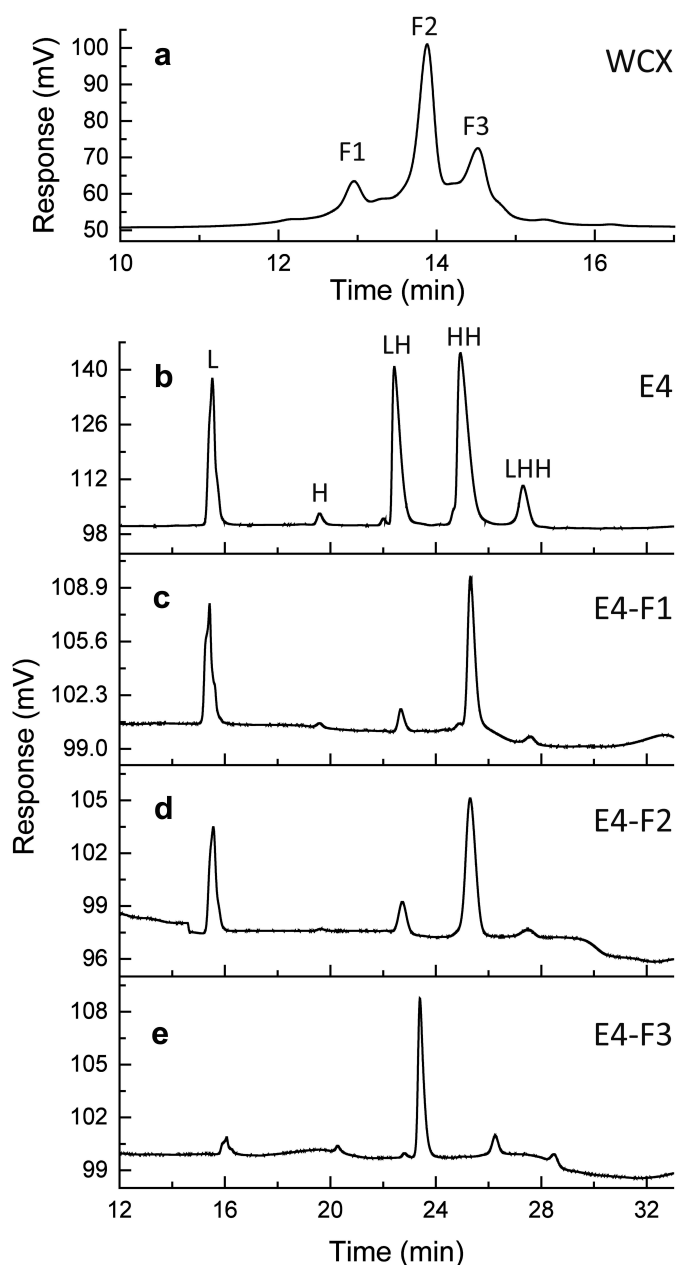
**Figure 4.** (a) Three WCX fractions collected for ADC1 E4; Non-reduced CE-SDS electropherograms for (b) ADC1 E4, (c) WCX Fraction 1, (d) WCX Fraction 2 and (e) WCX Fraction 3.

**Table 3.** Peak area percentages of fragments detected by non-reduced CE-SDS analyses for E2 and E4 species of ADC1 and ADC2 as well as their WCX fractions (WCX fractions of ADC1 E2 and E4 species were labeled in Figure 2 and those for ADC2 E2 and E4 species were labeled in Figure 3).

| Sample | Peak area% | | | | | | ID* |
|---|---|---|---|---|---|---|---|
| | L | H | LH | HH | LHH | LHHL | |
| ADC1 E2 | 15.1 | 0.4 | 0.4 | 2.8 | 75.9 | 5.4 | E2$_A$ |
| ADC1 E2 F2 | 15.2 | ND | ND | 7.3 | 74.7 | 2.8 | E2$_A$ |
| ADC1 E4 | 20.3 | 1.6 | 26.4 | 40.7 | 10.7 | 0.2 | |
| ADC1 E4 F1 | 32.6 | 1.0 | 5.5 | 58.6 | 2.3 | ND | E4$_{AA}$ |
| ADC1 E4 F2 | 29.0 | 0.5 | 9.7 | 56.6 | 4.1 | ND | E4$_{AA}$ |
| ADC1 E4 F3 | 9.2 | 2.6 | 72.6 | 11.0 | 4.7 | ND | E4$_{HH}$ |
| ADC2 E2 | 15.3 | 0.2 | 0.2 | 2.1 | 77.7 | 4.5 | E2$_A$ |
| ADC2 E2 F1 | 15.8 | ND | ND | 1.9 | 80.4 | 1.9 | E2$_A$ |
| ADC2 E4 | 20.2 | 1.0 | 29.9 | 40.0 | 8.9 | ND | |
| ADC2 E4 F1 | 27.3 | 0.8 | 10.5 | 57.0 | 4.4 | ND | E4$_{AA}$ |
| ADC2 E4 F2 | 7.7 | 1.7 | 68.2 | 10.7 | 11.7 | ND | E4$_{HH}$ |

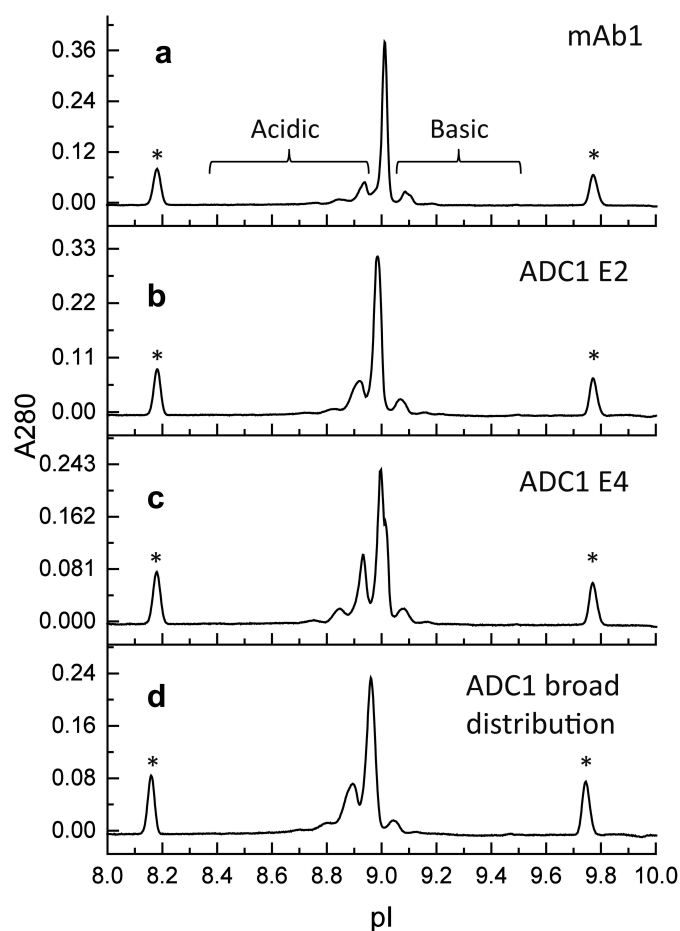*ID of main component
ND: not detected



**Figure 5.** icIEF electropherograms of (a) mAb1, (b) ADC1 E2, (c) ADC1 E4, (d) ADC1 broad distribution and (e) ADC1. Charge variants and percentages of charge variants are labeled for each sample. Only Lys0 peak was counted as main peak in each sample for comparison.

conjugation sites. A charged linker-drug, such as one containing MMAF, could further complicate the analysis by WCX. As a result, the peak compositions of an ADC with broad distribution separated by WCX are highly complex, and nearly every peak is a complex mixture of different charged species (acidic, main and basic) from certain positional isomers. Therefore, the percentage of the acidic and basic species detected by WCX for an ADC may not represent its true content of charge variants.

## Imaged capillary isoelectric focusing

icIEF was used to profile the charge variants in mAb1, ADC1, and its fractions. icIEF results are demonstrated in Figure 5. 4 M urea was used during sample preparation for better

reproducibility. In Figure 5, mAb1 and three ADC samples showed similar charge variants profile with similar pI values. Percentages of charge variants of ADC1 tested by icIEF are listed in Table 2. The pI values of the main peak in the mAb and three ADCs remained very close, which indicated that the majority of linker-drug mc-vc-MMAE was uncharged, and

barely changed the charge of the mAb before and after conjugation. In icIEF, the percentages of acidic species increased with increasing drug load, which are 21.4%, 27.6% and 33.8% for mAb1, ADC1 E2, and E4 species, respectively. Compared to the results from WCX (22.0%, 25.8% and 24.1% for mAb1, ADC1 E2, and E4, respectively), the trend, and particularly the percentage of acidic species in E4 species, are quite different. As reported in literature,[22] linker-drug mc-vc-MMAE could undergo succinimide ring hydrolysis and increase the acidity. In theory, with the increasing number of linker-drug per antibody, going from mAb1 to ADC1 E2 then to E4, the percentage of acidic species should increase in the order of mAb < E2 species < E4 species without other causes to change the charge distribution of the ADCs. Therefore, the results from icIEF agree more with the theoretical trend. Note that icIEF data of ADC1 with broad distribution was also easy to understand, as demonstrated in Figure 5d.
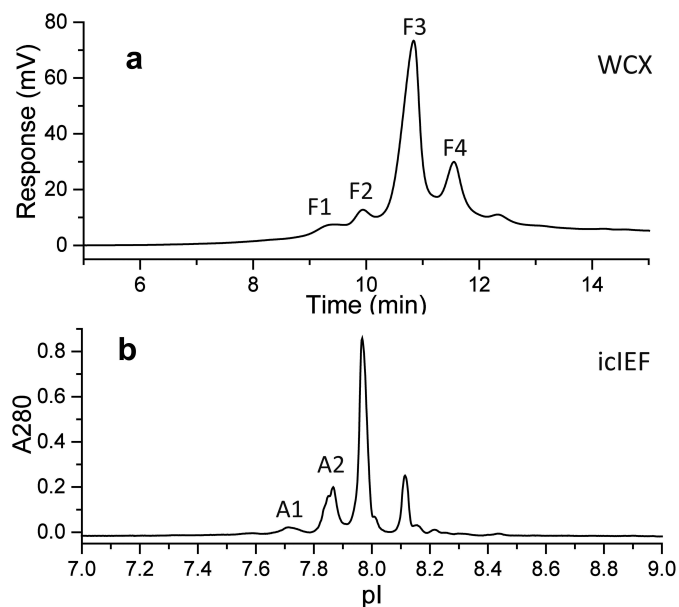


**Figure 6.** Analysis of ADC3 by (a) WCX and (b) icIEF. WCX fractions collected for subsequent analyses are illustrated. F1 = Fraction 1; F2 = Fraction 2; F3 = Fraction 3; F4 = Fraction 4; A1 = Acidic peak 1; A2 = Acidic peak 2.

### LC-MS peptide mapping of WCX fractions from ADC3

ADC3 was also analyzed by both WCX and icIEF, and its WCX profile was further characterized by peptide mapping. WCX and icIEF profiles for ADC3 look very similar, as illustrated in Figure 6. However, the two peaks in the acidic region showed different abundance when assessed using two different methods. In Figure 6, F1 and F2 in WCX were 13.0% in total by peak area, while A1 and A2 in icIEF accounted for 26.6% in total. Since ADC3 was a high purity ADC carrying two drugs at specific sites, the difference between the WCX and icIEF results was not caused by different drug loads or positional isomers. In order to understand the causes of charge variants in WCX, four fractions (as indicated in Figure 6) were collected during WCX analysis of ADC3 followed by LC-MS peptide mapping to check the charge-related modifications on mAb3 sequence and linker-drug. Based on the results, an asparagine deamidation on a peptide (peptide1) that contains an NG spot was the main contributor to acidity of F1 and F2 in WCX. As described in the methods section, we applied a low pH enzymatic digestion process to minimize deamidation artifacts in ADC3 from sample preparation. The levels of deamidated and non-deamidated forms in four fractions are illustrated in Figure 7. Other modifications such as deamination on other sites, oxidation, linker-drug hydrolysis, and off-target conjugation sites were also examined by peptide mapping. Based on the peptide mapping results, there was no significant difference between F1 and F2 considering charge-related modifications and positional isomers.

### Discussion

Here, we investigated WCX for its application in characterizing the charge variants of three ADCs. Significant differences were observed between mAb and ADC in WCX analyses with neutral linker-drug conjugated (Figures 2 and 3). The non-reduced CE-SDS results of WCX fractions in Table 3 indicated that WCX was capable of differentiating positional isomers in the ADCs analyzed in this study under native condition. Comparing HIC and WCX analyses of ADC1 and ADC2, HIC was effective in separating different drug load species of an ADC (E0, E2, E4, E6, E8), but it was not always able to differentiate positional isomers. On the other hand, WCX demonstrated good selectivity towards
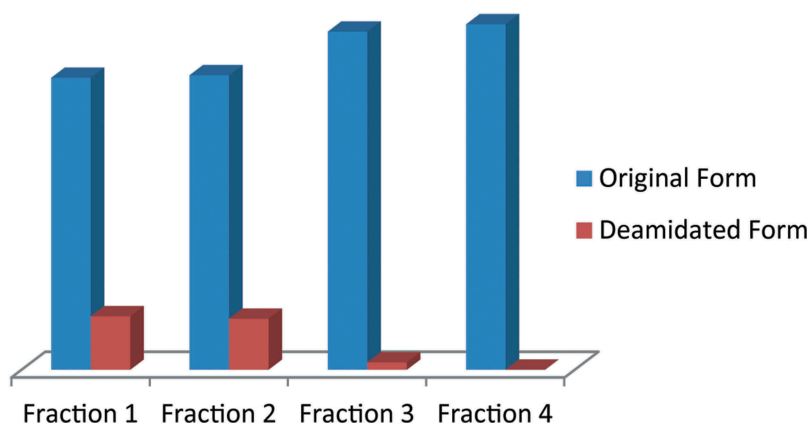


**Figure 7.** Percentage of variants of NG-containing peptide in ADC3.

positional isomers, but species with different drug loads could not be completely resolved. The unique selectivity of WCX demonstrated the potential of WCX to purify ADC positional isomers for in-depth studies.

Our results demonstrated that separation of ADCs in WCX mainly depends on three factors: 1) charge heterogeneity on the antibody, 2) drug load distribution,[17] and 3) the conjugation sites. For the two mc-vc-MMAE-conjugated ADCs (Figures 2 and 3), WCX exhibited limited resolution towards different drug loads, but good selectivity for positional isomers. As a result, multiple components in an ADC may coelute during WCX separation, especially for ADCs with higher drug load or broad distribution. This complexity potentially compromises the WCX's capability to quantify charge variants in ADCs.

The separation mechanism in IEX is complex. Although the primary driving force for separation is the difference in charge (overall charge and surface charge distribution), other types of interactions, such as hydrophobic interaction, hydrogen bond, and van der Waals interactions, can also lead to separation in the absence of charge differences.[11,23,24] The linker-drug mc-vc-MMAE in ADC1 and ADC2 does not carry a net charge. In Figure 2, ADC1 E2 and E4 species eluted earlier than mAb1, and the major peaks of ADC1 E2 and E4 were not obviously broader than the major peak in mAb1. Therefore, the hydrophobic interaction introduced by linker-drug (mc-vc-MMAE) was not significant on the TSKgel CM-STAT column, as hydrophobic interaction would usually delay elution and broaden the peak.[25,26] There were other effects introduced by the linker-drug that reduced the overall retention. Our hypothesis is that mc-vc-MMAE linker-drug may change the surface charge distribution on ADCs by interfering with the interactions between the amino acids around the conjugation sites and column stationary phase, and thus reduce the retention of the ADC. Comparing the two major peaks in ADC1 E4 (Figure 2), $E4_{AA}$ peak (F2) eluted earlier than the main peak in E2, while $E4_{HH}$ (F3) and E2 main peak had a similar retention time. This indicated mc-vc-MMAE linker-drug conjugated in the arm region (between the light chain and heavy chain) had a bigger impact to reduce the overall interaction between ADC1 and the WCX column than linker-drug conjugated in the hinge region (between two heavy chains), probably due to the higher solvent accessibility in the arm region.[1,3] Similar trends were observed for ADC2 in Figure 3.

icIEF profiles of ADC1 and ADC2 were consistent with their mAb profiles, which indicated linker-drug (mc-vc-MMAE) did not substantially interfere with the icIEF analyses. As a result, different profiles of the same ADC samples were observed between WCX and icIEF techniques. Even for ADC3, an ADC with controlled conjugation sites, a minor difference was still observed between WCX and icIEF analyses (Figure 6). Since no major differences in deamidation and other modifications were observed between the first two WCX fractions (F1 and F2) by peptide mapping, other factors such as conformation change may lead to the separation of F1 and F2. Furthermore, based on our experiences, linker-drugs that carry charges can further complicate both WCX and icIEF profiles of ADC.

Traditionally, IEX results match well with icIEF results for mAbs, allowing better understanding of charge variants profile.[6,13,27] However, the work shown here reveals that developing an IEX method with results aligned with icIEF results can be challenging for ADCs. Alternatively, novel techniques such as MS-compatible IEF[28] or 2D-CE[29] have emerged to aid interpretation of ADC charge variants.

Moreover, platform methods have increasingly drawn interest in the biopharmaceutical industry, with the goal of leveraging prior knowledge to accelerate CMC programs. Although IEX has been routinely used to analyze mAbs, it may not be practical to use the same method for an ADC. More considerations should be given to the specific properties of the compounds for method development. We hope our work brings some awareness to the ADC community of the need to select suitable techniques to analyze and characterize charge variants of ADCs.

## Materials and methods

### Materials

Three ADCs (ADC1, ADC2, and ADC3) were produced from three full-length humanized IgG1 monoclonal antibodies (mAb1, mAb2 and mAb3, respectively) developed within AbbVie. ADC1 and ADC2 have broad distribution and share the same linker-drug (mc-vc-MMAE). E2 and E4 (Table 1) fractions were collected for both ADC1 and ADC2 HIC for further analysis. ADC3 is a high purity E2 ADC (carrying two drugs) consisting of mAb3 and an AbbVie proprietary payload conjugated via a maleimide group.

### Hydrophobic interaction chromatography

HIC was used to profile the drug distribution of each ADC, and to confirm the purity of E2 and E4 fractions. Samples were injected onto a butyl-NPR column (4.6 mm x 3.5 cm, 2.5 μm, Tosoh Bioscience, King of Prussia, PA) and eluted with a gradient of mobile phase A (1.5 M ammonium sulfate in 25 mM sodium phosphate, pH 7.0) and mobile phase B (25 mM sodium phosphate pH 7.0:Isopropanol = 75:25). Flow rate was 0.8 mL/min, and column temperature was 30°C. An Agilent 1100 series HPLC system (Agilent Technologies, Palo Alto, CA) equipped with a diode array detector (DAD) was used. Signal was monitored at 280 nm.

### Weak cation exchange chromatography

An Agilent 1200 HPLC system with DAD and a fraction collector (Agilent Technologies, Palo Alto, CA) was used. A TSKgel CM-STAT (4.6 x 100 mm, 7 μm, Tosoh Bioscience, King of Prussia, PA) was used for WCX analysis. Mobile phase A was 20 mM MES, pH 6.5 and mobile phase B was 20 mM MES, 500 mM NaCl, pH 6.5. Gradient at a flow rate of 1.0 mL/min under 25°C was used to elute the sample and was varied for different ADCs. WCX fractions of ADCs were collected based on the retention time for further characterization. Signal was monitored at 280 nm.

## Capillary electrophoresis-sodium dodecyl sulfate

The ADCs and their WCX fractions were analyzed under denaturing and nonreducing conditions using a Beckman Coulter PA 800 Plus CE instrument (Beckman Coulter, Brea, CA). All reagents were from PA 800 plus IgG Purity/Heterogeneity Assay Kit and the method was used as described by the manufacturer. Briefly, about 100 ug ADC standard or 10 μL WCX fraction solutions diluted in 5 μL 500 mM iodoacetamide and sample buffer (not less than 50 μL) with final volume of 100 μL was heated at 70°C for 10 min. A bare-fused silica capillary with total length of ~30 cm, an inner diameter of 50 μm, and outer diameter of 375 μm was used for the separation and signals were monitored by a DAD at 214 nm. Sample was separated at −15 kV with reverse polarity. Peaks were assigned by their elution time as compared with elution times of intact antibody and light chain and heavy chain of fully reduced antibody. The peak elution order followed increasing molecular weight as light (L), heavy (H), light-heavy (LH), heavy-heavy (HH), light-heavy-heavy (LHH), and intact mAb/ADC (LHHL).

## Imaged capillary isoelectric focusing

A Protein Simple iCE3 instrument (Protein Simple, San Jose, CA) was used for the icIEF analysis of selected mAbs and their corresponding ADCs to compare with WCX analysis. mAb and ADC samples were analyzed following standard method from ProteinSimple using 50/50 Pharmalyte 3–10 (GE Healthcare, Little Chalfont, Buckinghamshire, UK)/Pharmalyte 8–10.5 (GE Healthcare, Little Chalfont, Buckinghamshire, UK). pI marker 8.18 and 9.77 were used to mark the pI range and urea was added in the sample to a final concentration to 4 M. The final protein concentration was around 2 mg/ml for each sample. For each icIEF analysis, sample was focused for 1 min at 1500 V followed by 10 min at 3000 V.

## LC-MS peptide mapping

The charge variant fractions of ADC3 were collected from WCX separation and analyzed by LC-MS peptide mapping. Fractions were first desalted and concentrated through an Amicon centrifugal filter (Millipore Sigma, Burlington, MA) to around 10 mg/mL. A previously reported method was followed for enzymatic digestion.[30] Briefly, reduction was conducted by adding 10 μL of ADC3 fractions to 140 μL of 10 mM TCEP in 6 M guanidine hydrochloride and 250 mM sodium acetate at pH 5.0 and incubating at 37°C for 15 min. The reduced ADC was then buffer exchanged to digestion buffer, which is 20 mM TrisHCl and 0.5 mM TCEP at pH 7.0. After that, 10 μg of Trypsin/LysC was added into reduced protein with 2-h incubation at 37°C. The digested WCX fractions of ADC3 were analyzed by an Acquity UPLC coupled to a Synapt G2 Si mass spectrometer (Waters, Milford, MA). Data analysis was performed by UNIFI software (Waters, Milford, MA). MS response derived from UNIFI was used for quantification of peptides and modified peptides.

## Abbreviations.

| | |
|---|---|
| ADC | Antibody-drug conjugate |
| AEX | Anion exchange chromatography |
| CE-SDS | Capillary electrophoresis sodium dodecyl sulfate |
| CEX | Cation exchange chromatography |
| cIEF | Capillary isoelectric focusing |
| CZE | Capillary zone electrophoresis |
| H | Heavy chain |
| HIC | Hydrophobic interaction chromatography |
| icIEF | Imaged capillary isoelectric focusing |
| IEX | Ion exchange chromatography |
| IgG | Immunoglobin gamma |
| L | Light chain |
| LC | Liquid chromatography |
| mAb | Monoclonal antibody |
| mc-vc-MMAE | Maleimidocaproyl-valine-citrulline-monomethyl auristatin E |
| MS | Mass spectrometry |
| WCX | Weak cation exchange chromatography |

## References

1. Wiggins B, Liu-Shin L, Yamaguchi H, Ratnaswamy G. Characterization of cysteine-linked conjugation profiles of immunoglobulin g1 and immunoglobulin g2 antibody-drug conjugates. J Pharm Sci. 2015;104:1362–72. doi:10.1002/jps.24338.
2. Le LN, Moore JM, Ouyang J, Chen X, Nguyen MD, Galush WJ. Profiling antibody drug conjugate positional isomers: a system-of-equations approach. Anal Chem. 2012;84:7479–86. doi:10.1021/ac301568f.
3. Sun MM, Beam KS, Cerveny CG, Hamblett KJ, Blackmore RS, Torgov MY, Handley FGM, Ihle NC, Senter PD, Alley SC. Reduction-alkylation strategies for the modification of specific monoclonal antibody disulfides. Bioconjug Chem. 2005;16:1282–90. doi:10.1021/bc050201y.
4. Wagner-Rousset E, Janin-Bussat MC, Colas O, Excoffier M, Ayoub D, Haeuw JF, Rilatt I, Perez M, Corvaïa N, Beck A. Antibody-drug conjugate model fast characterization by LC-MS following IdeS proteolytic digestion. MAbs. 2014;6:173–84.
5. M-C J-B, Dillenbourg M, Corvaia N, Beck A, Klinguer-Hamour C. Characterization of antibody drug conjugate positional isomers at cysteine residues by peptide mapping LC–MS analysis. J Chromatogr B. 2015;981-982:9–13. doi:10.1016/j.jchromb.2014.12.017.
6. Kaschak T, Boyd D, Lu F, Derfus G, Kluck B, Nogal B, Emery C, Summers C, Zheng K, Bayer R, et al. Characterization of the basic charge variants of a human IgG1: effect of copper concentration

in cell culture media. MAbs. 2011;3:577–83. doi:10.4161/mabs.3.6.17959.

7. Lee HJ, Pardridge WM. Monoclonal antibody radiopharmaceuticals: cationization, pegylation, radiometal chelation, pharmacokinetics, and tumor imaging. Bioconjug Chem. 2003;14:546–53. doi:10.1021/bc0256648.

8. Perkins M, Theiler R, Lunte S, Jeschke M. Determination of the origin of charge heterogeneity in a murine monoclonal antibody. Pharm Res. 2000;17:1110–17.

9. Hintersteiner B, Lingg N, Zhang P, Woen S, Hoi KM, Stranner S, Wiederkum S, Mutschlechner O, Schuster M, Loibner H, et al. Charge heterogeneity: basic antibody charge variants with increased binding to Fc receptors. MAbs. 2016;8:1548–60. doi:10.1080/19420862.2016.1225642.

10. Singh SK, Narula G, Rathore AS. Should charge variants of monoclonal antibody therapeutics be considered critical quality attributes? Electrophoresis. 2016;37:2338–46. doi:10.1002/elps.201600078.

11. Du Y, Walsh A, Ehrick R, Xu W, May K, Liu H. Chromatographic analysis of the acidic and basic species of recombinant monoclonal antibodies. mAbs. 2012;4:578–85. doi:10.4161/mabs.21328.

12. Hong G, Bazin-Redureau MI, Scherrmann JM. Pharmacokinetics and organ distribution of cationized colchicine-specific IgG and Fab fragments in rat. J Pharm Sci. 1999;88:147–53. doi:10.1021/js970335n.

13. Khawli LA, Goswami S, Hutchinson R, Kwong ZW, Yang J, Wang X, Yao Z, Sreedhara A, Cano T, Tesar DB, Nijem I. Charge variants in IgG1: isolation, characterization, in vitro binding properties and pharmacokinetics in rats. MAbs. 2010;2:613–24. doi:10.4161/mabs.2.6.13333.

14. Moorhouse KG, Nashabeh W, Deveney J, Bjork NS, Mulkerrin MG, Ryskamp T. Validation of an HPLC method for the analysis of the charge heterogeneity of the recombinant monoclonal antibody IDEC-C2B8 after papain digestion. J Pharm Biomed Anal. 1997;16:593–603.

15. Harris RJ, Kabakoff B, Macchi FD, Shen FJ, Kwong M, Andya JD, Shire SJ, Bjork N, Totpal K, Chen AB. Identification of multiple sources of charge heterogeneity in a recombinant antibody. J Chromatogr B Biomed Sci Appl. 2001;752:233–45.

16. Wakankar A, Chen Y, Gokarn Y, Jacobson FS. Analytical methods for physicochemical characterization of antibody drug conjugates. MAbs. 2011;3:161–72. doi:10.4161/mabs.3.2.14960.

17. Kubota K, Kobayashi N, Yabuta M, Ohara M, Naito T, Kubo T, OTSUKA K. Validation of capillary zone electrophoretic method for evaluating monoclonal antibodies and antibody-drug conjugates. CHROMATOGRAPHY. 2016;37:117–24. doi:10.15583/jpchrom.2016.011.

18. Michels DA, Salas-Solano O, Felten C. Imaged capillary isoelectric focusing for charge-variant analysis of biopharmaceuticals. Bioprocess Int. 2011;9:48–54.

19. Redman EA, Mellors JS, Starkey JA, Ramsey JM. Characterization of intact antibody drug conjugate variants using microfluidic capillary electrophoresis–mass spectrometry. Anal Chem. 2016;88:2220–26. doi:10.1021/acs.analchem.5b03866.

20. Henley WH, He Y, Mellors JS, Batz NG, Ramsey JM, Jorgenson JW. High resolution separations of charge variants and disulfide isomers of monoclonal antibodies and antibody drug conjugates using ultra-high voltage capillary electrophoresis with high electric field strength. J Chromatogr A. 2017;1523:72–79. doi:10.1016/j.chroma.2017.07.059.

21. Liu H, Chumsae C, Gaza-Bulseco G, Hurkmans K, Radziejewski CH. Ranking the susceptibility of disulfide bonds in human IgG1 antibodies by reduction, differential alkylation, and LC-MS analysis. Anal Chem. 2010;82:5219–26. doi:10.1021/ac100575n.

22. Shen B-Q, Xu K, Liu L, Raab H, Bhakta S, Kenrick M, Parsons-Reponte KL, Tien J, Yu S-F, Mai E, Li D. Conjugation site modulates the in vivo stability and therapeutic activity of antibody-drug conjugates. Nat Biotech. 2012;30:184–89. doi:10.1038/nbt.2108.

23. Kopaciewicz W, Rounds MA, Fausnaugh J, Regnier FE. Retention model for high-performance ion-exchange chromatography. J Chromatogr A. 1983;266:3–21. doi:10.1016/S0021-9673(01)90875-1.

24. Melander WR, El Rassi Z, Horváth C. Interplay of hydrophobic and electrostatic interactions in biopolymer chromatography: effect of salts on the retention of proteins. J Chromatogr A. 1989;469:3–27. doi:10.1016/S0021-9673(01)96437-4.

25. Yamamoto S, Nakanishi K, Matsuno R. Ion-exchange chromatography of proteins. CRC Press. 1988;43:1–33.

26. Gu B, Li Y, Lee ML. Polymer monoliths with low hydrophobicity for strong cation-exchange capillary liquid chromatography of peptides and proteins. Anal Chem. 2007;79:5848–55. doi:10.1021/ac0623585.

27. Liu H, Ren W, Zong L, Zhang J, Wang Y. Characterization of recombinant monoclonal antibody charge variants using WCX chromatography, iCIEF and LC-MS/MS. Anal Biochem. 2019;564-565:1–12. doi:10.1016/j.ab.2018.10.002.

28. Wang L, Bo T, Zhang Z, Wang G, Tong W, Da Yong Chen D. Da Yong Chen D. High resolution capillary isoelectric focusing mass spectrometry analysis of peptides, proteins, and monoclonal antibodies with a flow-through microvial interface. Anal Chem. 2018;90:9495–503. doi:10.1021/acs.analchem.8b02175.

29. Kohl FJ, Montealegre C, Neusüß C. On-line two-dimensional capillary electrophoresis with mass spectrometric detection using a fully electric isolated mechanical valve. Electrophoresis. 2016;37:954–58. doi:10.1002/elps.201500579.

30. Yu XC, Joe K, Zhang Y, Adriano A, Wang Y, Gazzano-Santoro H, Keck RG, Deperalta G, Ling V. Accurate determination of succinimide degradation products using high fidelity trypsin digestion peptide map analysis. Anal Chem. 2011;83:5912–19. doi:10.1021/ac200750u.